MASS LOSS FROM T TAURI STARS*

L. V. KUHI†
Lick Observatory, Mount Hamilton, California
Received June 20, 1964

ABSTRACT

The broad emission lines of H and Ca II in the spectra of T Tauri stars have been interpreted in terms of a simplified model for the mass-loss phenomenon assumed to be taking place. The expanding envelope is taken to be spherically symmetric, with the ejected atoms all having the same initial velocity and subjected only to gravitational forces. The emitting volume, essentially an H II region, is surrounded by an absorbing shell moving radially outward that produces the violet-displaced absorption components. A fit of computed line profiles to observed contours then gives the particle density at the surface of the star. This value combined with estimates of the stellar temperature and radius gives the present rate of mass loss. For six representative stars with varying emission-line strengths these rates range from 0 3 to 5.8 $\times$ 10^{-7} $m_{\odot}$ year^{-1}, with an average of 3.7 $\times$ 10^{-8} $m_{\odot}$ year^{-1}. No definite mechanism is proposed for the mass ejection, although it seems reasonable that a flux of high-energy protons postulated to account for the large extent of the ionized envelope may also be indirectly responsible for the ejection.

From the statistics of T Tauri stars, it is estimated that at any one time approximately 40 per cent of the contracting stars may be losing mass. A preliminary analysis of the effect of mass ejection on the time scale of the contraction, making use of Iben's theoretical tracks, indicates that mass ejection may be of some significance. Although it produces only about a 10 per cent decrease in the contraction time, the energy involved may at times be comparable to the radiated luminosity. Furthermore, a 1.0-$m_{\odot}$ star may altogether lose as much as 0 4 $m_{\odot}$, a non-negligible amount. It would seem that the effect of mass ejection should be considered in future computations of evolutionary tracks.

I. INTRODUCTION

T Tauri stars are now generally regarded as being young stars still in the contractive stage of evolution. Their peculiar spectral characteristics, irregular light variations, and other properties have recently been reviewed by Herbig (1962). The strongest emission lines (hydrogen and Ca II H and K) are as much as 5–6 Å wide and often have shortward-displaced absorption features with velocities ranging from -80 to -230 km/sec, indicating the presence of material moving away from the star. There is no sign of the return of this rising material, so the inference is drawn that it actually leaves the star, being driven in some manner from below since the line displacements usually do not exceed the velocity of escape at the stellar surface. Herbig (1961) has suggested that the forbidden lines observed in the spectra of most T Tauri stars arise in a circumstellar envelope supplied in this fashion.

No detailed analysis of the amount of material ejected has been carried out, although two rough estimates have been made. Varsavsky (1960) determined the rate of mass loss for T Tau to be about one solar mass in 10^7 years, by making use of the expansion velocity from the emission lines and the nebular density determined by Osterbrock (1958) from the relative intensities of the [O II] $\lambda\lambda$ 3727, 3729 doublet. Herbig (1960, 1962) has made estimates for LkHα 120, a very luminous T Tauri star with intense P Cygni-like structure in its emission lines. From an elementary theory of the P Cygni phenomenon together with an estimate of the effective temperature and luminosity, he obtained a value of one solar mass in 10^5 years for the rate at which material is rising from the surface of the star.

In addition, direct photographs of LkHα 120 (see Fig. 1) and T Tau show bright nebulosity in the immediate vicinity of the stars. LkHα 120 has a fringe of nebulosity fanning out from one side to a distance of 4″, and still further away (at 10″–25″, a linear

* *Contributions from the Lick Observatory*, No. 170.

† Present address: Mount Wilson and Palomar Observatories, Carnegie Institution of Washington, California Institute of Technology, Pasadena.

distance of 0.1–0.3 pc) is surrounded by an elliptical shell of nebulosity which may be the interface of material streaming out from the star and the surrounding cloud of gas and dust. T Tauri is also surrounded by nebulosity extending to several seconds of arc from the star, an envelope in which the forbidden lines of [S II], [O II], and [O I] are probably produced. It is tempting to think that this nebulosity is fed by ejected material from the star.

The T Tauri stars also undergo extremely irregular variations in light, changes of several magnitudes in a short period of time being not at all unusual (Kholopov 1954, 1961; Badalian 1958). This irregular variation suggests some form of random activity at the surfaces or in the atmospheres. We propose to consider the mass-ejection phenomenon further by attempting to reproduce the observed emission-line profiles for a number of T Tauri stars in terms of a simplified model for an expanding envelope of ejected material. The effect of such mass ejection on the contractive stage of stellar evolution will be estimated.

II. THE OBSERVATIONAL MATERIAL

The stars selected for study were chosen primarily for their accessibility to high-dispersion observations. This usually meant that they were observed at or near maximum light. Although only six stars were studied, the data still cover a fairly large range in spectral characteristics, particularly in the intensity of the emission lines.

TABLE 1

T TAURI STARS OBSERVED

Star	α (1900)	δ (1900)	Spectral Type*	Class†	m_{pg}
RY Tau .	$4^h15^m.8$	+28° 12′	dG0e	2	9 3–12 3
T Tau . .	4 16 2	+19 18	dG5e	2	9 6–13.5
GW Ori . . .	5 23 6	+11 47	dK3e	(2)	10 8–11 5
RU Lup . .	15 50.1	−37 32		5	9 6–13.4
AS 209 . . .	16 43.6	−14 13		4 u	12
LkHα 120 . .	20 57.9	+49 58	. .	4 *pec*	12.9

* Joy (1945)

† Herbig's emission-line intensity class

High-dispersion spectrograms for the six stars (see Table 1) covering the wavelength region from λ 3300 to λ 5000 and/or from λ 5300 to λ 6900 were kindly made available by Dr. G. H. Herbig. Most of these were taken with the 20-inch camera of the coudé spectrograph of the Lick 120-inch reflector at a dispersion of 16 Å/mm. In addition a few spectrograms had been taken at a dispersion of 10 Å/mm with the Mount Wilson 100-inch coudé spectrograph for which line profiles derived by Dr. K. Hunger were available. The detailed data concerning these plates are given in Table 2. The plate quality varied considerably, the spectra often being very narrow or even unwidened (as for LkHα 120 and AS 209) because of the faintness of the stars. In most cases, however, they were adequate to yield intensity profiles for the stronger emission lines (Hα, Hβ, Hγ, Hδ, Ca II H and K), although very little could be done with the stellar absorption features. Representative spectra are shown in Figures 2, 3, and 4 along with those of standard G- and K-type dwarfs.

The plates were calibrated photometrically by means of either a spot sensitometer or a step-slit arrangement. Direct-intensity tracings were obtained with the Lick microphotometer, used in conjunction with a Moseley Autograph curve-follower and a strip-chart recorder. A tracing of Ca II K of RY Tau is shown in Figure 5 to illustrate the amount of scatter due to grain and other factors which was later averaged out visually

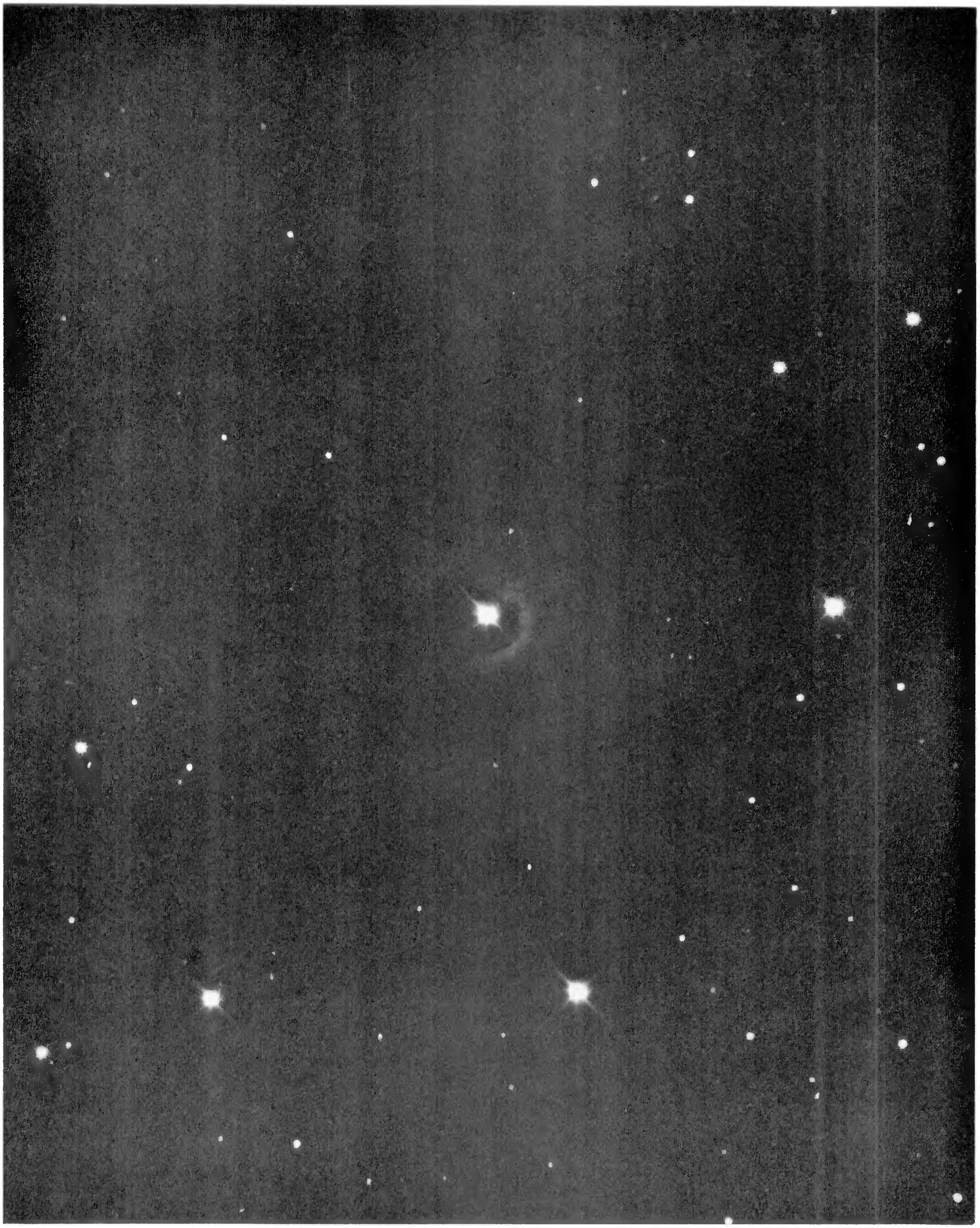

FIG. 1.—Direct photograph of the shell around LkHα 120. The original negative shows that there is bright material very close to the star, which is here lost in the overexposed star image. The original negative was taken by Dr. G. H. Herbig with the 120-inch reflector; the scale of the reproduction is 2.4″/mm; south is above and east to the right.

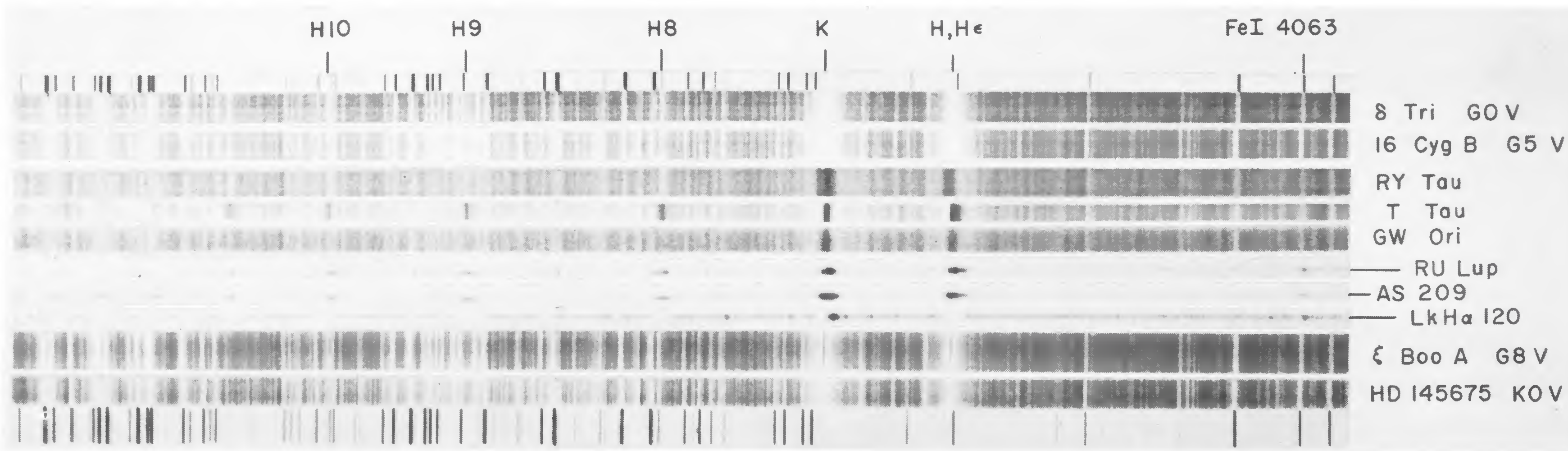

FIG. 2.—Spectra of T Tauri stars in the 3700–4100-Å region, with normal G-type dwarfs for comparison. All the spectra were taken with the 120-inch reflector; the details for the T Tauri spectra are given in Table 2.

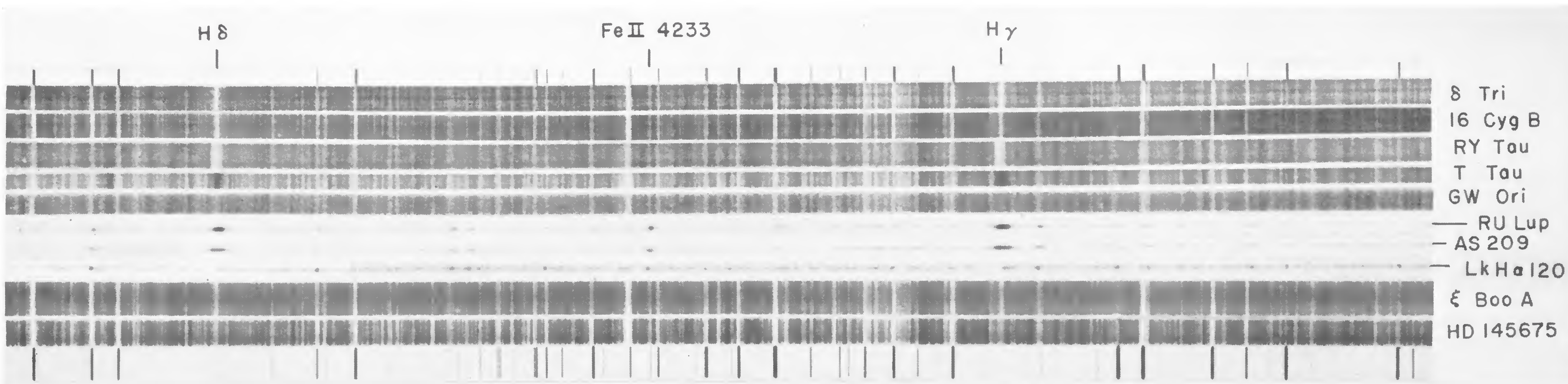

FIG. 3.—Spectra of T Tauri stars in the 4030–4450-Å region, with normal G-type dwarfs for comparison. All the spectra were taken with the 120-inch reflector; the details for the T Tauri spectra are given in Table 2.

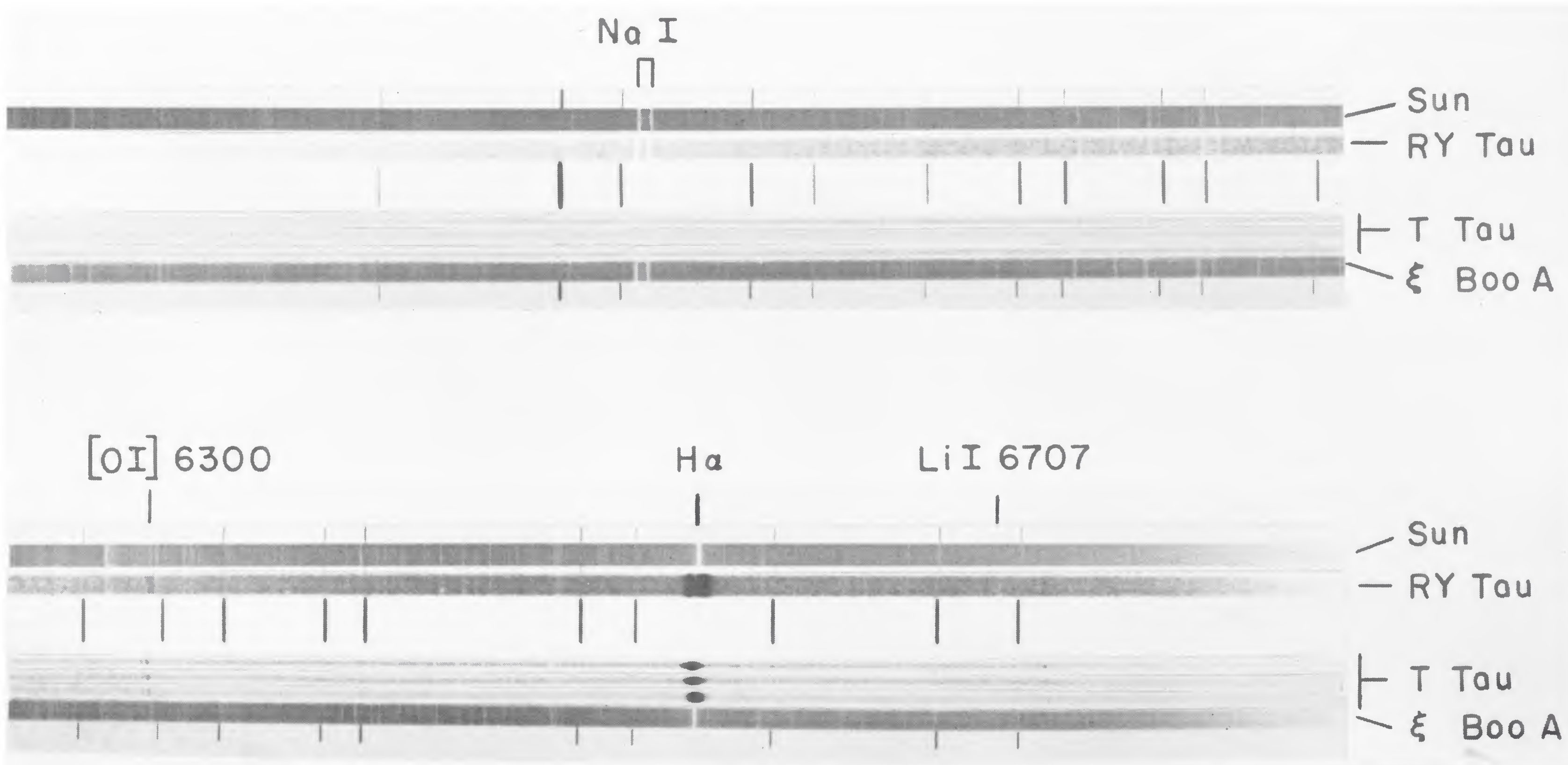

FIG. 4.—Spectra of T Tauri and RY Tauri, together with two normal G-type dwarfs, in the yellow-red region. (The line very near the position of Li I λ 6707 in the solar spectrum is not due to lithium, but to two other lines at λλ 6703, 6705.)

TABLE 2

PLATE DATA

Star and Plate No	Disper-sion (Å mm⁻¹)	Date	Exposure Time (min)	Emulsion (Kodak)	Measured Radial Velocity* (km/sec)
RY Tau:					
Ce 4882†	10	Sept. 29, 1947	302	103a-E+IIa-O	
EC 1519	32	Oct. 21, 1962	168	103a-F	.
EC 1520	16	Oct. 21, 1962	137	103a- O	+21
T Tau:					
Ce 4537†	10	Jan. 10, 1947	221	103a-E+IIa-O	..
EC 370	16	Oct. 30, 1960	156	103a-O	+17
EC 950.	16	Oct. 22, 1961	180	103a-O	..
EC 1351	16	Aug. 15, 1962	146	103a-F	. .
EC 1435	16	Sept. 13, 1962	222	103a-F	.
EC 1529	16	Oct. 22, 1962	176	103a-F	. ..
EC 1530	16	Oct. 22, 1962	126	103a-O	+20
EC 1531	16	Oct. 22, 1962	44	103a-F	.. .
EC 1532	16	Oct. 22, 1962	11	103a-F	.
GW Ori:					
EC 1680‡	16	Dec. 11, 1962	226	103a-O	+18
RU Lup:					
EC 44..	16	Mar. 20, 1960	50	103a-O	... ..
EC 1247	16	June 21, 1962	123	103a-O	..
AS 209:					
EC 588 .	16	Apr. 3, 1961	236	103a-O	.. ..
EC 660	16	May 22, 1961	190	103a-O	.. ..
LkHα 120:					
EC 174 .	16	July 6, 1960	160	103a-O	.. ..

* Joy (1945) determined the mean radial velocity of T Tau and RY Tau to be +25 and +26 km/sec, respectively.

† Mount Wilson plates by R F. Sanford

‡ Lick plate by G W Preston

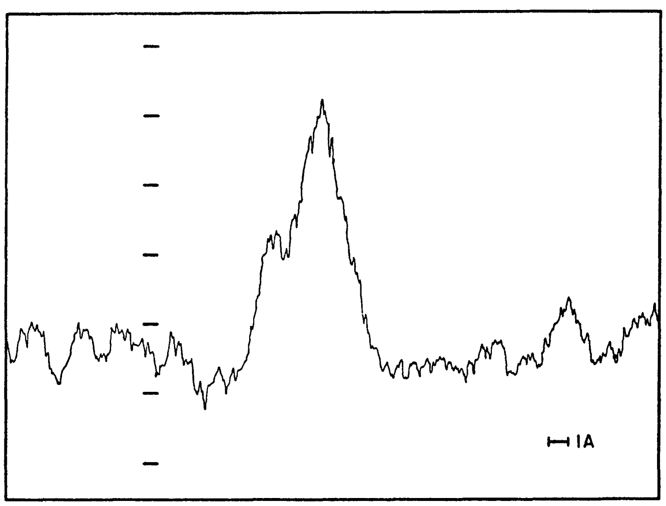

FIG. 5.—Direct intensity tracing of Ca II K in RY Tauri, showing the amount of grain fluctuations

in obtaining the profiles used in the computations. The relative magnitude of the fluctuations varies considerably depending on the width of the spectrum.

Wherever possible, the absorption spectra were also measured for radial velocity on the basis of wavelengths recommended by Wright (1951). The results are listed in Table 2. The velocities indicated on the profiles are all with respect to the stellar absorption features. In the diagrams illustrating the emission profiles (see Figs. 7–10) the solid curve always indicates the observed contour and the dashed curve the contour computed from the theory now to be described.

III. THE MODEL

a) *The Emission Features*

The problem of emission lines produced by moving envelopes has been discussed by various authors, particularly for Wolf-Rayet and P Cygni stars. Rottenberg (1952) considered a hot star that emitted a continuous spectrum, enclosed by an expanding envelope in which emission lines are formed by resonance scattering. Rublev (1961), following Sobolev (1960), investigated the emission and absorption components separately and paid special attention to the geometrical factors connected with the velocity distribution in the envelope and its thickness. He obtained line profiles for matter moving with constant and with increasing velocity. Chandrasekhar (1934) has considered in detail the geometry of the situation; because of the inherent simplicity of his picture and the fact that the envelope of a T Tauri star may not be excited solely by thermal radiation, the following discussion will be based on his approach.

Following Chandrasekhar, consider the atoms to be leaving the stellar surface all with some initial velocity v_0 directed uniformly radially outward from the star of radius R_0. The atom is subjected to a deceleration due to gravity so that at some value of $r = r_2$ the velocity $v = 0$ if $v_0 < v_\infty$, thus forming the outer boundary of the envelope. If $v_0 \geq v_\infty$ the envelope would theoretically extend to infinity, but long before this condition is reached the interaction with the surrounding interstellar material would provide a limiting radius.

From the equation of motion we get

$$v(r) = \left(v_0^2 + \frac{R_0}{r} - 1\right)^{1/2}, \tag{1}$$

where $v_\infty = (2gR_0)^{1/2}$ has been used as a unit of velocity (in cm/sec) and r (in cm) is the radial coordinate measured from the center of the star. The equation of continuity gives

$$\rho(r) = \rho(R_0)\,\frac{R_0^2 v_0}{r^2(v_0^2 + R_0/r - 1)^{1/2}}, \tag{2}$$

where $\rho(R_0)$ is the density at $r = R_0$.

Assume now that the emission cm^{-3} is proportional to the square of the density (on the assumption that most of the hydrogen in the envelope is ionized so that $N_\epsilon \approx N_i \approx N_{\text{H}}$) and can be represented by

$$i(r) = \epsilon \rho^2 v^\beta, \tag{3}$$

the v^β term insuring that $i(r) \rightarrow 0$ as $v \rightarrow 0$ to avoid the resulting singularity at $r = r_2$.

Then the total emission at any point $\Delta\nu = u v_\infty \nu / c$ (where $u = v \cos\theta$ is also measured in terms of v_∞) in the profile is given by

$$i(u)\,du = 2\pi \int\!\!\int i(r) r^2 \sin\theta d\theta dr, \tag{4}$$

where the integration is to be carried out over the surface of constant radial velocity (see Fig. 6 for the geometry of the model and a constant radial-velocity surface) and the envelope is assumed completely transparent in the Balmer-line radiation. Transforming equation (4) into an integral involving only θ yields

$$i(u) = k' u^{\beta-1} \int_{\theta_1}^{\theta_2} \sec^{\beta}\theta \sin\theta \, d\theta \,, \tag{5}$$

where

$$k' = 4\pi\epsilon\rho^2(R_0)R_0^3 v_0^2 \tag{6}$$

and ϵ is a constant factor of proportionality. The limits θ_1 and θ_2 will be different for the longward and shortward sides of the profile because of occultation effects due to the finite size of the stellar disk. In particular, for some value of $u \leq u_{\rm red}$ all the emission on the red side will be lost, because the constant radial-velocity surface lies behind the star. The limits are determined graphically by plotting u versus $u \sec \theta$ as discussed by Chandrasekhar (1934, which see for details). On the violet side the limits are $\theta_1 = 0$ and

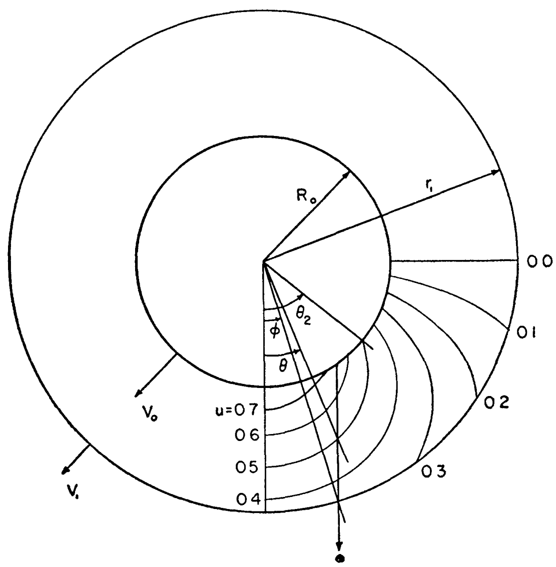

FIG. 6.—Geometry of the model, and the constant-velocity (u) surfaces for $v_0 = 0.8$. R_0 is the radius of the star, r_1 that of the absorbing layer, and $R_0 \rightarrow r_1$ the extent of the emitting region; v_0 is the velocity of ejection, and v_1 that of the absorbing layer.

$\theta_2 = \cos^{-1}(u/v_0)$ if the emission extends to $r = r_2$, or $\cos\theta_1 = u(v_0^2 + R_0/r_1 - 1)^{1/2}$ and $\cos\theta_2 = u/v_0$ if it extends only to $r = r_1 < r_2$.

If the ejection is actually represented by this scheme, it is obvious that the profiles will be asymmetrical and that this asymmetry will be given by $u_{\rm red}/v_0$. Since no velocity dispersion has been asumed, $u_{\rm red}$ represents the longward width of the line measured from the undisplaced frequency and v_0 the shortward width. Chandrasekhar also gives $u_{\rm red}$ and $u_{\rm red}/v_0$ as a function of v_0 so that the escape velocity can also be determined and thus the effective gravity g, and hence a lower limit on the mass of the star provided the stellar radius is known.

Since none of the observed profiles shows the flat tops to be expected when $v_0 > v_\infty = 1$, we restrict ourselves to $v_0 < v_\infty$, even though this does introduce the following serious problem. If $v_0 < v_\infty = 1$ the material cannot be expected to leave the star completely, and so it should eventually return unless some other forces act. In the T Tauri stars observed, no sign of this returning material, if it exists, is present in the spectra. Thus we are forced to think of the matter as being constantly pushed outward by the pressure of the material rising below it, so that in this case the problem is hydrodynamic rather than ballistic.

The possibility might also be considered that the ejected material is accelerated as it leaves the star somewhat in the manner of a solar wind. In this case the profiles take on a distinctly different appearance (see also Chandrasekhar 1934). In particular the two wings of the emission lines would be of equal width since the high velocities would not now be affected by occultation. Instead the central regions of the line are modified in the sense that the shortward side at low velocities will be more intense than the corresponding longward side. Thus the line will be asymmetrical but in the opposite sense from the case of deceleration which produces wings of different width. Most of the observed profiles show asymmetry of the latter type so that deceleration would seem to be indicated. However, for T Tau itself an acceleration could fit the observations as well, so that there is no clear-cut choice. Simply to be consistent we shall proceed with the decelerated case. However, it may be that as mass ejection subsides in a solar-type star it comes to resemble a solar wind–type phenomenon in which accelerating forces play a dominant role.

b) The Absorption Features

The observed line profiles are often deeply mutilated by overlying absorption features which must also be explained by the model. To do so, assume that the emitting region is still completely transparent to the line radiation but in addition that it is surrounded by a thin shell of radius $r = r_1$, of optical thickness $\tau = N'\alpha$ (where N' is the number of absorbing atoms cm^{-2} in the line of sight and α is the absorption coefficient per atom) moving with a velocity v_1 radially outward from the star. In the case of hydrogen assume also that no further emission occurs for $r > r_1$. The atoms in the shell will have a spread in velocity characterized by Δv_D, which will have both thermal and turbulent components.

Now at each value of θ the difference in radial velocity Δu between an emitting atom on the constant radial-velocity surface u and an absorbing atom in the shell $u_1 = v_1 \cos \phi$ will be different, i.e., the absorption is a function of θ. Thus the intensity at any θ will be

$$i(u) = k' u^{\beta-1} \int_{\theta_1}^{\theta_2} \sec^{\beta}\theta \sin\theta \exp[-\tau(\theta)]\, d\theta , \tag{7}$$

where

$$\tau(\theta) = N'_{n'}\alpha_0 \exp[-(\Delta u/\Delta v_D)^2] , \tag{8}$$

the thickness of the shell being infinitesimal, and

$$\begin{aligned} N'_{n'} &= \text{number of atoms cm}^{-2} \text{ in the lower state } n', \\ \alpha_0 &= \frac{\pi^{1/2} e^2 \lambda f_{n'n}}{m c \Delta v_D} , \\ \Delta u &= u - v_1 \cos\phi , \end{aligned} \tag{9}$$

where we have assumed a Maxwellian velocity distribution of absorbing atoms in the shell and pure Doppler broadening. We obtain $\cos\phi$ from Figure 6 as

$$\cos\phi = \left[1 - \left(\frac{r \sin\theta}{r_1}\right)^2\right]^{1/2} , \tag{10}$$

where

$$r = R_0/(u^2 \sec^2\theta - v_0^2 + 1) . \tag{11}$$

Equation (7) then gives the intensity of the radiation from the emitting region after it has passed through the absorbing shell. The light from the photosphere undergoes a similar absorption which must also be considered:

$$i_c(u) = \int I'_{c\nu}(\theta) \exp[-\tau(\theta)]d\theta , \quad (12)$$

where $I'_{c\nu}$ is the emission cm^{-2} of the stellar surface and $\tau(\theta)$ is given by equation (8) as before. Thus the total intensity at any point $\Delta\nu = uv_\infty\nu/c$ in the profile in terms of the continuum intensity is

$$I(u) = \frac{1}{I_{c\nu}} \left\{ k' u^{\beta-1} \int_{\theta_1}^{\theta_2} \sec^\beta\theta \sin\theta \exp[-\tau(\theta)]d\theta + \int_{\substack{\text{star}\\ \text{disc}}} I'_{c\nu}(\theta) \exp[-\tau(\theta)]d\theta \right\} \quad (13)$$

$$= \frac{1}{I_{c\nu}} k' u^{\beta-1} \int_{\theta_1}^{\theta_2} \sec^\beta\theta \sin\theta \exp[-\tau(\theta)]d\theta + \exp(-\tau) \quad (14)$$

if limb-darkening is neglected, and since $\cos\phi \approx 1$ over the stellar disk (because the angle subtended by it at $r = r_1$ is very small), $\tau \neq \tau(\theta)$ so that $i_c(u) = I_{c\nu} \exp(-\tau)$ where $I_{c\nu}$ is the total continuous radiation received from the stellar surface. Equation (14) for $I(u)$ was integrated numerically.

We then have the following parameters to be determined directly from the profile:

$N'_{n'}$ = number of atoms in the lower state n',

Δv_D = dispersion of absorbers in radial velocity,

v_1 = expansion velocity of absorbing shell, given directly by the velocity of the observed absorption component,

v_0 = ejection velocity at the surface,

v_∞ = escape velocity,

k' = a constant containing various atomic and stellar parameters (see below), dependent on the intensity.

c) Determination of Density $\rho(R_0)$ from k'

The value of k' is determined empirically by adjustment of the above-mentioned parameters until the best fit to the observed profile is obtained. In order to determine the density at the stellar surface, k' must be related to the atomic and stellar parameters. Consider first the Balmer lines: it can readily be shown that the energy emitted cm^{-3} for transitions from level n to n' is given by (see standard discussions such as that by Aller 1956)

$$E_{nn'} = \frac{N_i N_\epsilon K Z^4}{T_\epsilon^{3/2}} b_n \frac{g}{n^3 n'^3} 2hRZ^2 \exp X_n , \quad (15)$$

where the notation is standard, and the N's are particles cm^{-3}. It has been assumed earlier that $E_{nn'}$ is proportional to the square of the density which implies that $N_i \approx N_\epsilon$; this is true if the chief constituent of the envelope is ionized hydrogen.

In determining the value of k' from the emission line, the intensity was measured in terms of the adjacent continuum $I_{c\nu}$. If this can be represented by the Planck formula

$$I'_{c\nu} d\nu = \frac{2h\nu^3}{c^2} (e^{h\nu/kT} - 1)^{-1} d\nu \quad (16)$$

and

$$I_{c\nu}\, d\nu = 4\pi R_0^2 I'_{c\nu}\, d\nu , \quad (17)$$

we have

$$k' = 4\pi\epsilon\rho^2(R_0)R_0^3 v_0^2 \text{ per unit velocity interval or}$$

$$= 4\pi\epsilon\rho^2(R_0)R_0^3 v_0^2 \frac{\lambda}{v\infty} \text{ per unit frequency interval and}$$

$$\epsilon = \frac{KZ^4}{T_\epsilon^{3/2}} b_n \frac{g}{n^3 n'^3} 2hRZ^2 \exp X_n, \tag{18}$$

so that

$$\frac{k'}{I_{c\nu}} = \frac{\rho^2(R_0)R_0^3 v_0^2 \lambda KZ^4}{I'_{c\nu} v\infty T_\epsilon^{3/2}} b_n \frac{g}{n^3 n'^3} 2hRZ^2 \exp X_n, \tag{19}$$

from which $\rho(R_0)$ may be obtained, provided that the electron temperature T_ϵ and the temperature T of the star itself are known; for the latter, the effective temperature has been used.

We will further assume that the b_n's are those given by Menzel and Baker for Case B (Baker and Menzel 1938), the envelope being optically thick in both the Lyman continuum and line radiation. Burgess (1958) has recomputed the b_n's taking into account the l-degeneracy of the energy levels; his results differ at most by 30 per cent from Baker and Menzel's. This, however, does not introduce any error in the final result comparable to the uncertainties involved in the determination of the stellar temperatures and radii. It is recognized that these nebular b_n's are not strictly appropriate for the present situation, but they are used in the absence of a detailed study of conditions in this envelope.

For the Ca II K-line the only essential difference lies in the expression for $E_{nn'}$, the energy emitted cm^{-3}. Again, using the standard notation

$$E_{nn'} = \left(\frac{T_i}{T_\epsilon}\right)^{1/2} \frac{a_{\text{Ca}} N_{\text{H}} N_\epsilon}{x} \left(\frac{h^2}{2\pi m k}\right)^{3/2} \frac{\varpi_n}{2u_i} \frac{1}{T_\epsilon^{3/2}} f_{n'n} \frac{8\pi e^2 \nu^3 h}{m c^3} \exp \frac{I - \chi_n}{kT_i}, \tag{20}$$

where

$$a_{\text{Ca}} = \text{relative abundance of calcium to hydrogen,}$$

$$N_{\text{H}} = \text{number density of hydrogen particles}$$

$$= \frac{N_i x}{a_{\text{Ca}}} = \frac{N_{\text{III}}}{a_{\text{Ca}}} \left(\frac{1}{x_1 x_2} + \frac{1}{x_2} + 1 + \ldots\right),$$

where x_i = relative degree of ionization, and N_{III} = number of doubly ionized calcium atoms. Thus $\epsilon = E_{nn'}/N_{\text{H}}N_\epsilon$ for the Ca II K-line provided that a_{Ca} and x are known. We assume that the Ca/H ratio is equal to that in the Sun and then with a suitable temperature estimate the electron density. This discussion has involved the tacit assumption that the temperature in the emitting volume is not a function of θ or r. Since the volume is essentially an H II region, this does not seem at all unreasonable. In the use of equation (20) it has been assumed that the ionization (T_i) and electron (T_ϵ) temperatures are both equal to 9000° K.

d) The Rate of Mass Loss

When the densities at the surface are known, the instantaneous rate of mass loss can be estimated since the radius of the star is determined from its effective temperature and luminosity (see below) and the ejection velocity is given by the observed profile. The present rate of mass loss is

$$\frac{dm}{dt} = 4\pi R_0^2 N_{\text{H}}(R_0) v_0 m_{\text{H}}, \tag{21}$$

where v_0 is now in cm/sec and m_{H} is the mass of the hydrogen atom.

The total mass of the envelope is

$$m_{\text{env}} = 4\pi m_{\text{H}} \int_{r=R_0}^{r'} \rho(r) r^2 dr , \tag{22}$$

where $\rho(r)$ is given by $N_{\text{H}}(r)$ and the upper limit is to be determined. We must consider two cases depending on the value of v_0.

(i) $v_0 = v_\infty = 1$:

$$m_{\text{env}} = 4\pi m_{\text{H}} N_{\text{H}}(R_0) R_0^{3/2} \cdot \tfrac{2}{3}(r'^{3/2} - R_0^{3/2}) . \tag{23}$$

In this case the envelope theoretically extends to infinity so that $m_{\text{env}} \to \infty$ as $r \to \infty$; however, we shall assume that r' will be given by the value of r at which v becomes small, say 10 km/sec, i.e., $r' = R_0/(v^2 - v_0^2 + 1) = R_0/v^2$ where $v = 10/v_\infty$.

(ii) $v_0 < v_\infty = 1$:

Let $y = 1/r$; then

$$m_{\text{env}} = -4\pi m_{\text{H}} N_{\text{H}}(R_0) R_0^2 v_0 \int \frac{dy}{(v_0^2 + R_0 y - 1)^{1/2} y^2} , \tag{24}$$

which can be integrated directly:

$$m_{\text{env}} = [4\pi m_{\text{H}} N_{\text{H}}(R_0) R_0^2 v_0] \left\{ \frac{(v_0^2 + R_0 y - 1)^{1/2}}{(v_0^2 - 1) y} + \frac{R_0}{2(v_0^2 - 1)} \left[\frac{2}{(1 - v_0^2)^{1/2}} \tan^{-1} \left(\frac{[v_0^2 + R_0 y - 1]^{1/2}}{(1 - v_0^2]^{1/2}} \right) \right] \right\} , \tag{25}$$

where $r' = r_1$ for the mass inclosed by the emitting region or $r' = r_2$ for the total mass of the envelope.

If the ejection is continuous over a time large compared to the time t_R required to completely replace the envelope, then we can determine a representative value for t_R from the present rate of mass loss by dividing the results for m_{env} from equations (23) or (25) by the rate from equation (21).

IV. COMPUTATIONS AND RESULTS

The data for each star are given below, but a few general remarks are first in order. The line profiles used result from visual smoothing of the microphotometer tracings and are thus subject to personal bias. However, the salient features should be represented with adequate accuracy. The intensities are all given in units of the adjacent continuum.

Because of the assumptions of the model, we can hope to explain only the grosser features. In particular, since it has been assumed that all the emitting atoms have the same velocity, we cannot expect to reproduce the low-intensity wings which are present in most of the contours; it seems rather unlikely that the star ejects atoms uniformly over its entire surface with the same initial velocity, especially if the acceleration mechanism is similar to that operating in solar flares. Any departures from uniformity will lead to discrepancies between the observed and computed profiles. However, since we are primarily interested in the average number of atoms leaving the surface per second, these deviations in the detailed structure need not be of major concern.

The uncertainties of the effective temperatures and radii of the stars constitutes one of the largest sources of error. To determine the effective temperatures, reliable $B - V$ colors and/or spectral classifications are needed. The $B - V$ data which does exist is very meager and must be corrected for unknown amounts of reddening and absorption of both interstellar and circumstellar origin. In addition, the UBV colors are contaminated by both line and continuous emission. An attempt to avoid the contamination of the B-filter by emission lines was made recently by Smak (1964) for some stars in the Taurus cloud by changing the band pass of the filter so as to avoid the most prominent contributors $H\beta$ and $H\gamma$. Also a more quantitative estimate of the contamination of the U and the B by emission was determined spectrophotometrically for AS 209 by Kuhi (unpublished). AS 209 has a very large ultraviolet excess so that corrections for less-extreme stars could be scaled down from the factors for AS 209. These results were used in estimating effective temperatures and radii from the UBV colors and magnitudes. The results are given in Table 3.

The spectral type is difficult to obtain in T Tauri stars because of the broadened absorption features and in particular because of the filling in by the blue continuum. Often no stellar absorption lines are even visible. Stars such as T Tau and RY Tau for which classifications from low dispersion already exist (Joy 1945) seem to have been given too early a spectral type. Recent narrow-band photoelectric photometry by Wood

TABLE 3

DETERMINATION OF EFFECTIVE TEMPERATURES AND RADII

Star	M_v*	$(B-V)$*	$M_{\rm bol}$	T_e (° K)	$R_0/R_\odot$
RY Tau ..	+3 73	+0.99	3 30	4400	3.25
T Tau .	3 35	1 08	2 81	4100	4.56
GW Ori ..	1 7	1 01	1 27	4250	8 64
RU Lup	4.0	1 0	3 58	4270	2.95
AS 209. .	4 33	1.09	3 78	4090	2 94
LkHα 120 .	0 21	0 79	0 04	4960	11 2

* The M_v and $(B-V)$ have been corrected for interstellar absorption and for contamination by emission (see text).

(1963) indicates a later spectral type than G5 for T Tau, and high-dispersion spectra by Herbig give a value of K1. Thus one cannot rely very strongly on the temperatures obtained from the older spectral types. For this reason and also because no type could be assigned to three of the stars due to the absence of stellar absorption features, the colors were used almost exclusively together with the relations between $B-V$, bolometric correction, and effective temperature compiled by Schwarzschild (1958). It has also been assumed that the absorption is equal in all cases, i.e., $A_v = 0.9$ mag. and $E_{B-V} = 0.30$ (for a true distance modulus of 6.1 mag. for the Taurus cloud), and that the correction for the effect of the emission lines on $B-V$ is $+0.10$ mag. This procedure is open to considerable error for obvious reasons.

If the bolometric magnitude $M_{\rm bol}$ and the effective temperature T_e can be obtained in this way, the radius is obtained from

$$L = 4\pi R_0^2 \sigma T_e^4 , \qquad (26)$$

where

$$\log \frac{L_*}{L_\odot} = \frac{1}{2.5}(M_{\rm bol\odot} - M_{\rm bol*}) \qquad (27)$$

with $L_\odot = 3.78 \times 10^{33}$ erg/sec and $M_{\rm bol\odot} = +4.63$, so that

$$\log \frac{R_0}{R_\odot} = \tfrac{1}{2} \log L_* - 9.268 - 2 \log T_e . \qquad (28)$$

The individual circumstances of the stars observed are as follows.

1. *RY Tauri.*—RY Tau is located at the head of a faint fan-shaped nebula about 7′ in length. However, no nebulosity such as is observed very close to T Tau has been detected (Herbig 1961). Joy (1945) originally classified the star as F8 to G0, although Lick high-dispersion plates indicate that it is as late as G5. The H- and K-emission lines and the four lower members of the Balmer series are the only ones seen with any great strength, those of Ca II varying considerably with time. Overlying absorption features have been noted at −75, −90, −96 km/sec in three different years (Herbig 1958). The stellar absorption lines are fairly broad, indicating a $v \sin i \approx$ 45–50 km/sec (Herbig 1957). The color variation has been observed photographically by Badalian (1958) and the light-curve by Kholopov (1954, 1961). The light variations are never rapid, although there are more fluctuations near maximum light.

2. *T Tauri.*—T Tau illuminates NGC 1555, a reflection nebula which has long been known for its variability, and in addition is surrounded by a very small variable shell (Joy 1945; Herbig 1950) which has already been mentioned. The spectral type of T Tau is dG5e according to Joy and K1 according to Herbig. Bright Na I D-lines have been observed by Sanford (1947), accompanied by absorption at −165 km/sec similar to the displaced absorption components of the hydrogen and calcium lines. These absorption features have been noted at varying velocities and are sometimes even double, e.g., −43, −203 km/sec and −97, −142 km/sec on two different occasions. However, on the present plates the Na I D-lines show no emission and the velocity displacement of the absorption features is −140 km/sec with no indication of a second component. The stellar absorption lines lead to a $v \sin i \approx$ 20 km/sec (Herbig 1957). The star undergoes erratic changes in brightness; its light-curve has been studied by Kholopov (1954) and its color variations by Badalian (1958). Weston and Aller (1955) have noted extremely rapid fluctuations in the line structure over a period of a few hours. Babcock (1958) has found no evidence for a magnetic field and concluded that any existing field must be less than 1000 gauss.

3. *GW Orionis.*—GW Ori is a T Tauri-like star showing emission only at Hα, Ca II H and K, and possibly at Hβ. Its spectral type according to Joy (1949) is dK3e. Its light range is 0.7 mag., which is rather small compared to many T Tauri stars.

4. *RU Lupi.*—The spectrum of RU Lup is that of an advanced T Tauri star. There is no stellar absorption spectrum visible so that a spectral type has not been assigned.

5. *AS 209.*—AS 209 shows an intense emission spectrum, the strongest lines being those of H and Ca II. Weaker lines of Fe II, Fe I, Ti II, Mg I, [O II], and [S II] also appear, but the forbidden lines are very weak. No stellar absorption lines can be seen. The star has a very large ultraviolet excess which is most likely due to Balmer-line and continuous emission. The corrected color leads to a spectral type of about dK3e. No light variations have been observed. The star illuminates faint nebulosity.

6. *LkHα 120.*—The nebulosity of rather complex structure in which LkHα 120 is imbedded has already been discussed. The spectrum of the star itself is of advanced T Tauri–type, but its strongest lines show an exaggerated P Cygni–like structure, mentioned earlier; the strengths of the displaced hydrogen and Ca II absorption fringes are comparable to these lines in an F0–F2 dwarf. There has been no observed change in the spectrum over a period of 4 years, and no stellar absorption features are visible. An absolute magnitude near 0.0 makes it extremely luminous for a normal T Tauri star.

Summary of results.—The observed and computed profiles are shown in Figures 7–10; the numerical data are listed in Tables 4–9 and summarized in Tables 10 and 11. In general the profiles from several different plates of one star could all be fitted with the same values of the adjustable parameters, indicating that changes over the period covered by the observations are not large. The computed profiles, although representing the over-all shape of the lines, do not agree with the details as well as one might like. The differences might be due to density and/or velocity fluctuations in the envelope. The hydrogen and calcium lines both show this effect, although the departures from prediction occur at different points in the line on different plates. This fact implies fluctuations in time as well as in space. This is also borne out by the requirement of two absorbing layers in the cases of GW Ori, RU Lup, and LkHα 120 and the earlier observations of double absorption features in T Tau. However, some additional explanation is needed for T Tau in which the Ca II K-line is much too sharp for the computed profile and the higher members of the Balmer series result in consistently lower densities and require lower values of v_0. This suggests that the lines are not all formed throughout the same

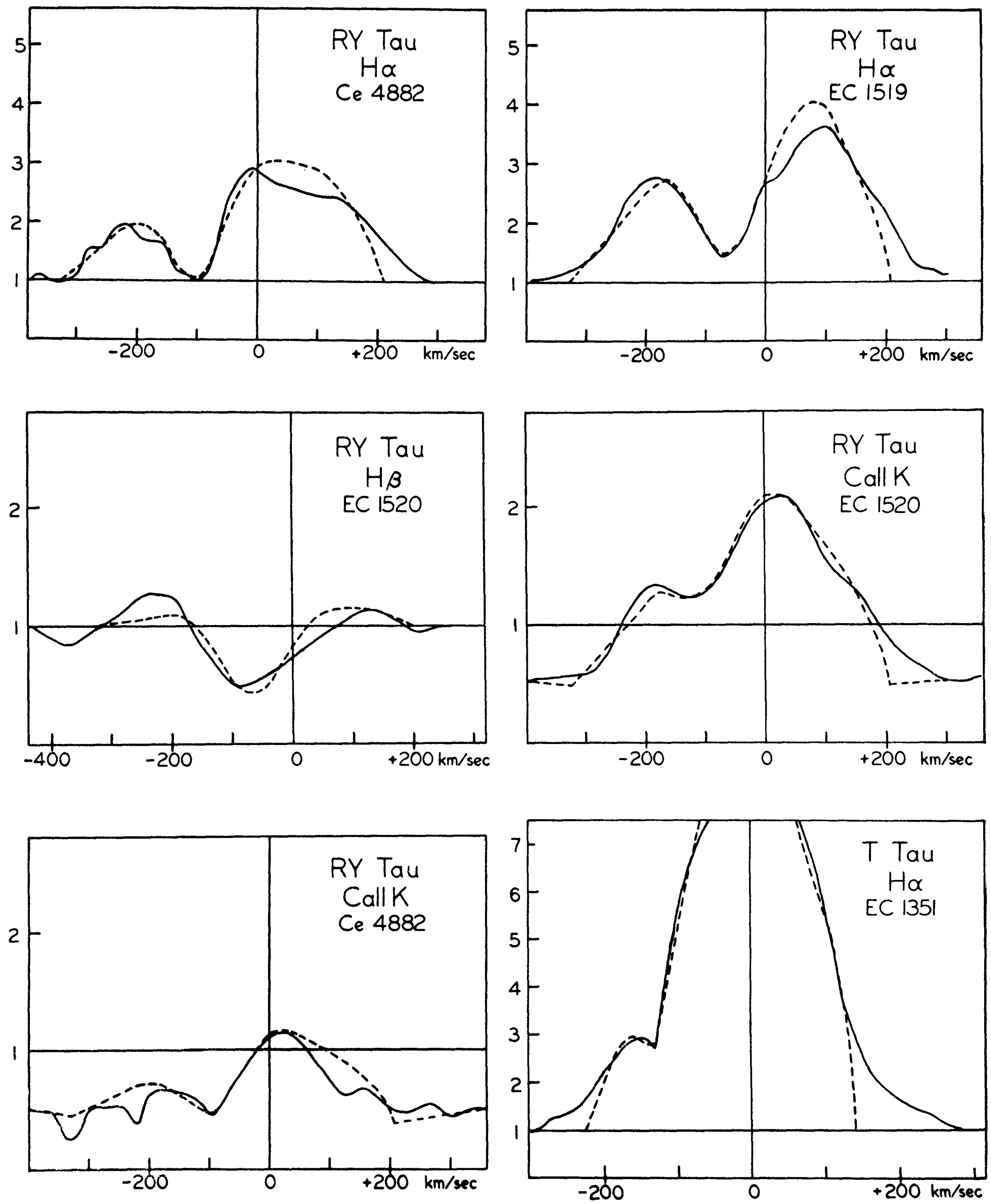

FIG. 7.—Observed (*solid curves*) and computed (*dashed curves*) line profiles in T Tauri stars

volume of the emitting region. The displaced absorption features indicate a fairly large velocity dispersion (30–110 km/sec) showing either a high degree of turbulence or a large radial velocity spread in the absorbing layer. The shell expansion velocities range from -80 to -200 km/sec with one exception: in AS 209 the absorption occurs at zero velocity, implying that the envelope extends to infinity or, more probably, that the ejected material has interacted with its surroundings and come to rest at some finite distance from the star.

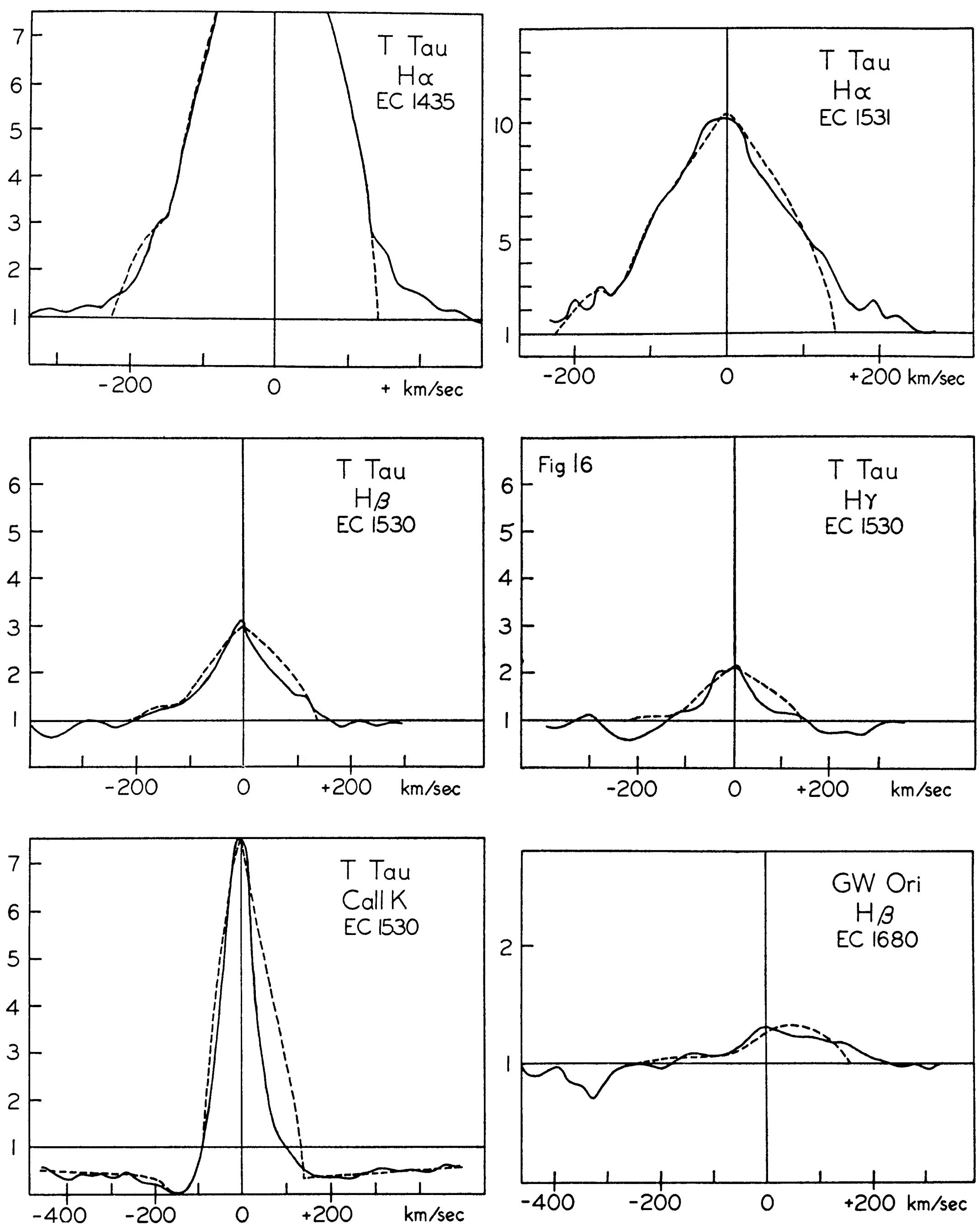

FIG. 8.—Observed (*solid curves*) and computed (*dashed curves*) line profiles in T Tauri stars

The ejection velocities range from 225 to 325 km/sec and from 0.7 to 1.0 times the escape velocity. The rates of mass loss are quite large, although for LkHα 120 the rate is smaller by an order of magnitude than Herbig's earlier estimate. However, they still indicate that a star could not undergo such ejection for any great length of time without substantially altering its mass (which is probably of the order of 1–2 $m_{\odot}$).

The replacement times, t_R, in Table 11 are relatively short, of the order of days and years, and not hundreds of years as previously suggested by Varsavsky (1960). This is

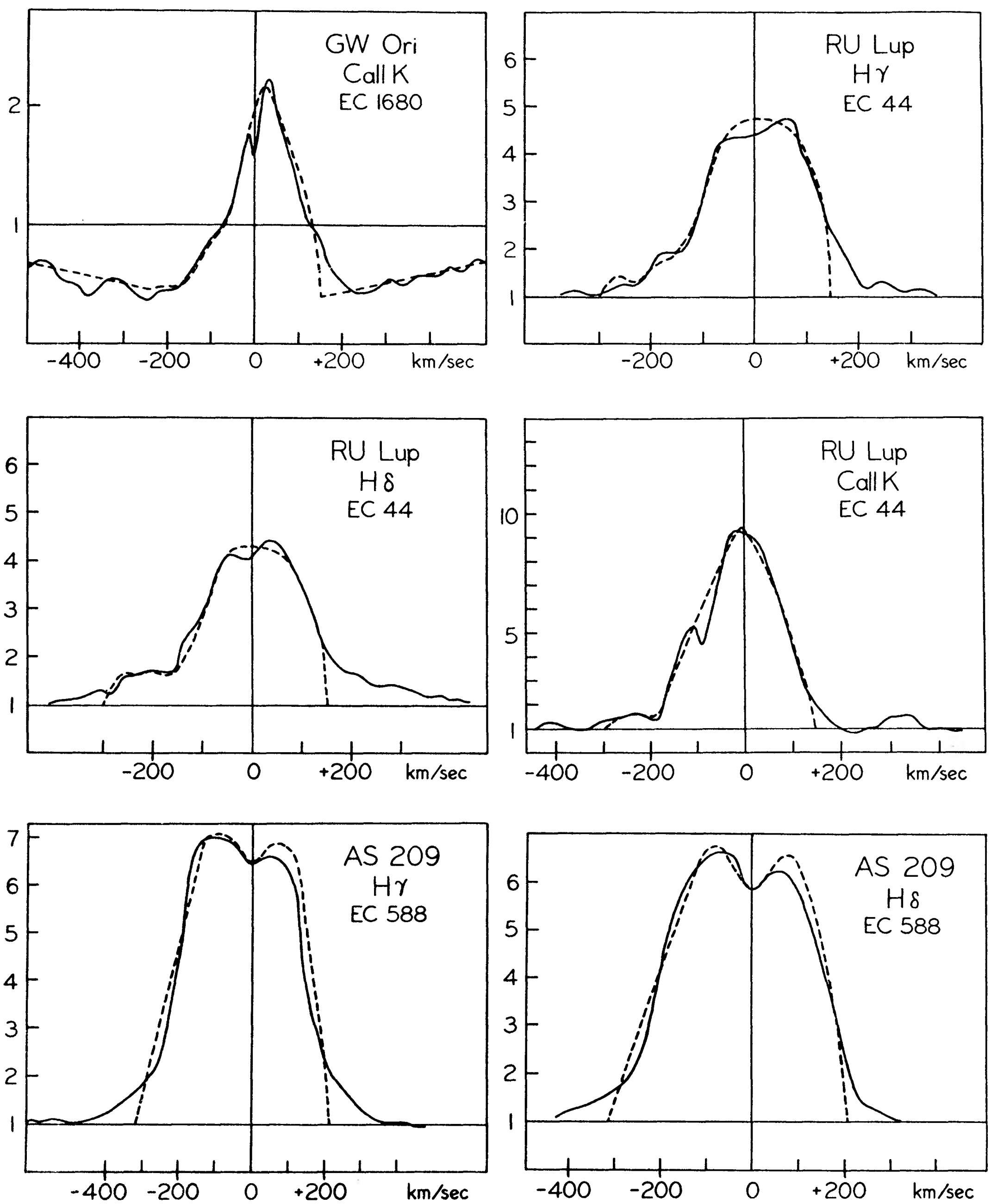

FIG. 9.—Observed (*solid curves*) and computed (*dashed curves*) line profiles in T Tauri stars

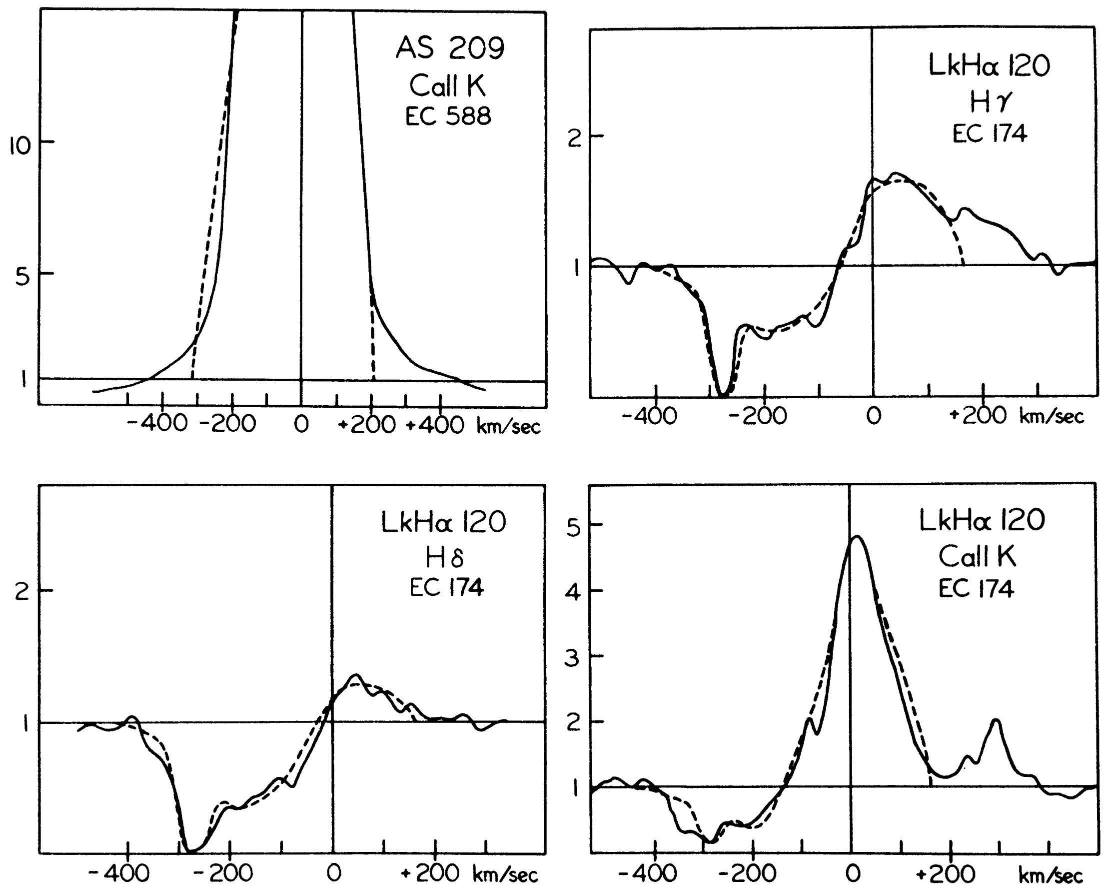

FIG. 10.—Observed (*solid curves*) and computed (*dashed curves*) line profiles in T Tauri stars

TABLE 4

RESULTS FOR RY TAURI

($r_1 = 10.52$ R$_0$, $r_2 \rightarrow \infty$; $v_0 = v_\infty = 325$ km/sec, $v_1 = 100$ km/sec)

PLATE	LINE	DENSITY $N_H(R_0)$ (10^{10} atom cm^{-3})	NO. OF ATOMS LOST PER CM^2 (10^{17} atom cm^{-2} sec^{-1})	MASS LOST BY ENTIRE STAR		$N'(r_1)$ (10^{13} cm^{-2})
				dm/dt (10^{18} gm sec^{-1})	dm/dt (10^{-7} $m_\odot$ yr^{-1})	
EC 1519 .	Hα	1.72	5.59	2 35	0 375	0.864
Ce 4882	Hα	1 48	4 81	2 07	332	0 864
EC 1520	Hβ	0 58	1 89	0.81	.130	6 9
EC 1520 .	Ca II K	1 51	4.90	1.85	.296	0.552
Ce 4882	Ca II K	0 90	2 91	3.12	0 498	0.414
Mean		1.19	3.87	1.96	0.314	

TABLE 5

RESULTS FOR T TAURI

($r_1 = 2.57\ R_0$, $r_2 \rightarrow \infty$; $v_0 = v_\infty = 225$ km/sec, $v_1 = 140$ km/sec)

Plate	Line	Density $N_H(R_0)$ (10^{10} atom cm^{-3})	No of Atoms Lost per Cm^2 (10^{17} atom cm^{-2} sec^{-1})	Mass Lost by Entire Star		$N'(r_1)$ (10^{13} cm^{-2})
				dm/dt (10^{18} gm sec^{-1})	dm/dt ($10^{-7}\ m_\odot$ yr^{-1})	
EC 1435	Hα	1.16	3 62	3 07	0 491	0 154
EC 1529	Hα	1 57	3 53	2 99	479	0 193
EC 1351	Hα	1 52	3 42	2 90	464	0 243
EC 1530	Hβ	0 828	1 86	1 58	253	
EC 1530	Hγ	0 699	1 60	1 35	216	
Ce 4537	Hγ	0 516	1 16	1 00	.160	.
EC 1530	Ca II K	1 22	2 75	2 33	372	4 94
Ce 4537	Ca II K	1 27	2 86	2 42	0 387	5 10
Mean		1 15	2 59	2 21	0 353	

TABLE 6

RESULTS FOR GW ORIONIS

($r_1 = 9.0\ R_0$, $r_2 \rightarrow \infty$; $v_0 = v_\infty = 240$ km/sec, $v_1 = 80$ km/sec)

Plate	Line	Density $N_H(R_0)$ (10^{10} atom cm^{-3})	No. of Atoms Lost per Cm^2 (10^{17} atom cm^{-2} sec^{-1})	Mass Lost by Entire Star		$N'(r_1)$ (10^{13} cm^{-2})
				dm/dt (10^{18} gm sec^{-1})	dm/dt ($10^{-7}\ m_\odot$ yr^{-1})	
EC 1680	Hβ	0 334	0 801	2 44	0 390	1 85
EC 1680 .	Ca II K	0 270	0 648	1.97	0 315	1 00
Mean		0 302	0 724	2 20	0 352	

TABLE 7

RESULTS FOR RU LUPI

($r_1 = 1.375\ R_0$, $r_2 = 1.96\ R_0$; $v_0 = 300$ km/sec, $v_\infty = 429$ km/sec, $v_1 = 200$ km/sec)

Plate	Line	Density $N_H(R_0)$ (10^{10} atom cm^{-3})	No of Atoms Lost per Cm^2 (10^{17} atom cm^{-2} sec^{-1})	Mass Lost by Entire Star		$N'(r_1)$ (10^{13} cm^{-2})
				dm/dt (10^{18} gm sec^{-1})	dm/dt ($10^{-7} m_\odot$ yr^{-1})	
EC 44	Hγ	6 88	20 6	7 31	1.17	1 86
EC 44	Hδ	9 36	28 1	9 95	1 59	3 98
EC 44	Ca II K	8 81	26 4	9 38	1 50	1 07
Mean		8 35	25 0	8 91	1 42	

TABLE 8

RESULTS FOR AS 209

($r_1 \rightarrow \infty$, $r_2 \rightarrow \infty$; $v_0 = v_\infty = 325$ km/sec, $v_1 = 0$)

Plate	Line	Density $N_H(R_0)$ (10^{10} atom cm^{-3})	No of Atoms Lost per Cm^2 (10^{17} atom cm^{-2} sec^{-1})	Mass Lost by Entire Star		$N'(r_1)$ (10^{13} cm^{-2})
				dm/dt (10^{18} gm sec^{-1})	dm/dt ($10^{-7} m_\odot$ yr^{-1})	
EC 588	Hγ	3 11	10 1	3 55	0 569	1 12
EC 588 .	Hδ	3 50	11 4	4 01	641	4 80
EC 588	Ca II K	4 09	13 3	4 69	0 750	
Mean		3 57	11 6	4 08	0 653	

TABLE 9

RESULTS FOR LkHα 120

($r_1 = 1.695$ R$_0$, $r_2 = 2.78$ R$_0$; $v_0 = 300$ km/sec, $v_\infty = 375$ km/sec, $v_1 = 180$ km/sec)

Plate	Line	Density $N_H(R_0)$ (10^{10} atom cm^{-3})	No of Atoms Lost per Cm^2 (10^{17} atom cm^{-2} sec^{-1})	Mass Lost by Entire Star		$N'(r_1)$ (10^{14} cm^{-2})
				dm/dt (10^{18} gm sec^{-1})	dm/dt ($10^{-7} m_\odot$ yr^{-1})	
EC 174	Hγ	2 38	7 14	36 2	5 79	5 11
EC 174	Hδ	2 01	6 03	30 6	4 89	10 95
EC 174	Ca II K	2 83	8 49	43 1	6 88	0 509
Mean		2 41	7 22	36 6	5 85	

TABLE 10

SUMMARY OF RESULTS

Star	v_1 (km/sec)	v_0 (km/sec)	v_∞ (km/sec)	$m/m_\odot$	Density $N_H(R_0)$ (10^{10} atom cm^{-3})	No of Atoms Lost per Cm^2 (10^{17} atom cm^{-2} sec^{-1})	Mass Lost by Entire Star	
							dm/dt (10^{18} gm sec^{-1})	dm/dt ($10^{-7} m_\odot$ yr^{-1})
RY Tau	100	325	325	0 90	1 19	3 87	1 96	0 31
T Tau	140	225	225	0 60	1 15	2 59	2 21	0 35
GW Ori	80	240	240	1 30	0 30	0 72	2 20	0 35
RU Lup	200	300	429	1 42	8 35	25 0	8 91	1 42
AS 209 .	0	325	325	0 81	2 57	11 6	4 08	0 65
LkHα 120	180	300	375	4 10	2 41	7 22	36 6	5 85

in line with the observed changes occurring over periods of the order of a decade as indicated by Herbig and others for the emission-line nebula surrounding T Tau. Herbig also suggested that this nebula would tend to be swept away continually by encounters of the nebular atoms with those of the surrounding cloud as the star passes through it. Some such mechanism is necessary for stars with $v_0 < v_\infty$ to avoid the piling-up of ejected material to such an extent that it becomes opaque to the continuous radiation of the star.

V. THE MAINTENANCE OF IONIZATION AND THE SOURCE OF EJECTION

The foregoing calculations yield a typical value of $R_0 \approx 3\, R_\odot$ for the star and $3\, R_0$ for the outer radius of the emitting envelope, which has an effective temperature of 4500° K. If the level of ionization in the envelope were maintained by stellar radiation, the resulting H II region surrounding the star would be quite small, having a thickness of about 2×10^8 cm, or $10^{-3}\, R_0$. Since the emitting volume is considerably larger, it is clear that some additional source of energy is required.

TABLE 11

INSTANTANEOUS MASS OF ENVELOPE, REPLACEMENT TIMES, AND COMPUTED RATES OF MASS LOSS

Star	Mass of Envelope*		Replacement Times		Emission-Line Intensity Class	dm/dt ($10^{-7}\, m_\odot$ yr^{-1})
	$m(r_1)$ (10^{22} gm)	$m(10)$ (10^{25} gm)	$t_R(r_1)$ (days)	$t_R(10)$ (days)		
RY Tau.	4.72	4.87	0 28	290	2	0 31
T Tau..	1 19	4.35	.062	230	2	0 35
GW Ori...	17.7	9.45	.93	500	(2)	0 35
RU Lup .	2.04	0.0037	.026	0 048	5	1 42
AS 209 ..	.....	1 08	....	31	4 u	0 65
LkHα 120	90 5	0.174	0 29	0 55	4 pec	5 85

* The $m(r_1)$ is the mass of the emitting region enclosed within the radius r_1; in the case of AS 209, the absorption feature occurs at zero velocity and $v = v_\infty$ so that this region would extend to infinity The $m(10)$ is the mass of the envelope out to some arbitrary radius determined by the velocity at which the material can be said to have actually left the star. This velocity has been chosen to be 10 km/sec

A possible source could be a flux of high-energy particles accelerated by a flare-type mechanism in the surface, which pass through the photospheric material and lose most of their energy in ionization and excitation processes. If the energy of recombination lost in line and continuous emission in the envelope ($E = 6.8 \times 10^{32}$ erg sec^{-1}) and the kinetic energy of the ejected material (9×10^{17} atom cm^{-2} sec^{-1}) is supplied by high-energy protons, the required particle flux can be estimated. The ionization and excitation must occur in the lower regions of the photosphere because the mean range of the protons is only about 2.5×10^5 cm. For proton energies of 3 MeV, the required flux is about 5×10^{14} particles cm^{-2} sec^{-1}, but whether the "observed" extent of the emitting region is compatible with these figures has not been investigated.

Since the total energy of the particles is considerable ($\sim$ 0.05 of the stellar luminosity) it is quite conceivable that their production by some flare-type mechanism could well be a means of releasing some of the magnetic energy stored in the star during formation (e.g., by the winding-up of magnetic lines of force as postulated by Hoyle 1960). Thus it is possible that the ejection of matter may be a somewhat indirect result of the star's attempt to reduce its angular momentum.

VI. EFFECT OF MASS LOSS ON THE CONTRACTION STAGE

As a first approximation to the effect of mass loss on the contraction time scale, we represent the luminosity L of the star as

$$L = a\,\frac{dR}{dt} - b\,\frac{dm}{dt}, \tag{29}$$

where $a dR/dt$ represents the energy supplied by contraction and $b dm/dt$ that carried away by mass loss, so that $b = v^2/2$, where v is the velocity of ejection at the surface. If the star were a polytrope of index n, then for the case of completely radiative equilibrium $n = 3$ and $a = 3\,G\,m^2/4R^2$; for the convective case $n = 1.5$ and $a = 3\,G\,m^2/7R^2$. However, since the actual situation is not so simple, the value of a is best determined from theoretical contraction tracks (Iben 1963) which include allowance for the development of a radiative core, the onset of nuclear burning, the development of a convective core, and a proper treatment of the nuclear-energy sources. Such tracks provide L, dR, and dR/dt as a function of time from some assumed initial configuration. Needless to say, if the effect of dm/dt is large, it must be included in the computations from the beginning, so that the present discussion could then be only a rough approximation.

Then, neglecting nuclear-energy sources (which presumably are not significant during the mass-ejection stage),

$$dt = \frac{a\,dR}{L + b\,dm/dt}, \tag{30}$$

so that

$$\tau = \int \frac{a\,dR}{L + b\,dm/dt}, \tag{31}$$

where τ is the modified contraction time. It is clear therefore that mass loss will shorten the time scale; i.e., the star loses energy both by radiation and mass ejection so that it evolves at a faster rate. The magnitude of the effect can be determined if we know dm/dt and its variation with time during contraction. We attempt to estimate the time variation of dm/dt from the statistics of T Tauri stars.

First, it is necessary to determine what fraction of contracting stars show the T Tauri phenomenon. If the irregular variables in the Orion Nebula can all be considered to be in the contraction stage, Herbig (1962) has estimated that the T Tauri stars comprise approximately 0.48 of the total variable-star population of the Nebula (for stars fainter than $m_{pg} = +12.0$ at maximum light). Walker (1956, 1957) has found the same fraction to be 0.36 for NGC 2264 and 0.41 for NGC 6530. Thus a value of 40 per cent for the fraction of contracting stars in the T Tauri stage of their evolution will be assumed.

The stars in the T Tauri stage can be further subdivided according to Herbig's emission-line intensity index which describes the over-all intensity of the emission lines relative to the continuum. It ranges from 1 for emission observed only at Hα to 5 for advanced T Tauri types having very strong H, Ca II, and relatively strong metallic emission. The "T Tauri–like" stars will usually be classified as 1 or 2. As shown in Table 11 and Figure 11, there is a fair degree of correlation between the present rate of mass loss as obtained in this investigation and the emission-line intensity index. Since the index classification is based on low-dispersion spectrograms and since a substantial variation with time can be expected for many stars, the degree of correlation indicated is perhaps all that could be expected.

We now make use of this correlation by considering Herbig's index as being indicative of the intensity of the activity that is responsible for the mass loss, and by using his list of known T Tauri stars brighter than $m_{pg} = +14.5$, we can obtain some idea of the number of stars in each class and thus estimate the number now undergoing mass ejection at a particular rate. This list is, of course, subject to selection effects in that the brighter stars along with those showing strong emission lines are more readily discovered and thus are more completely represented. Table 12 gives the number of stars in each emission class and the "average" rate of mass loss for each class as determined from the computed rates for five of the six stars observed. The sixth, LkHα 120, was not included because of the peculiar nature of its spectrum and its apparent high luminosity. The value for class 1 is only an estimated upper limit on the rate, which in reality may be negligible since the only observed emission is at Hα. Such emission could easily arise from flare and prominence activity that may involve little mass loss.

From the histogram (Fig. 12) it is quite clear that most of the stars have quite low rates of mass loss: i.e., less than 0.50×10^{-7} solar masses per year. From Table 12, assuming the average rates for each class to apply and weighting according to the population in each class, we find an over-all mean rate of ejection equal to 3.7×10^{-8} $m_\odot$ year^{-1} for the T Tauri stage.

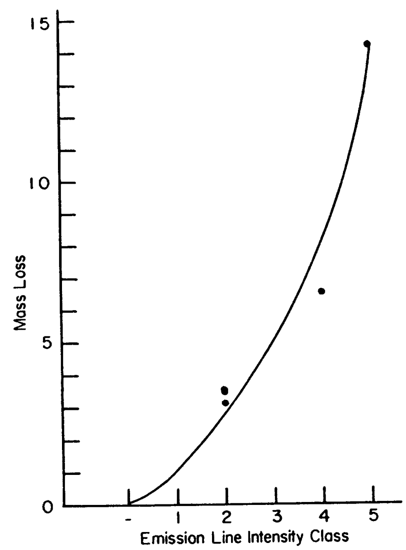

FIG 11.—Mass loss (in solar masses per 10^7 years) as a function of Herbig's emission-line intensity class, as determined in this investigation.

TABLE 12

AVERAGE RATES OF MASS LOSS

Emission-Line Intensity Class	No of Stars	Fraction of Stars	Average Rate of Mass Loss (10^{-7} $m_\odot$ yr^{-1})
5	7	0 02	1 40
4	19	0 06	0 80
3	30	0 10	0 50
2	35	0 11	0 30
1	33	0 11	0 10
	186	0 60	0 00
Total	310	1 00	

We now assume that the present number of stars in each class is proportional to the time that a star spends in that class. This implies that all contracting stars go through each stage of emission although not necessarily in the order suggested by the classes; the time scale of existing observations is, of course, not long enough to permit any direct conclusion. In addition, the distribution among the classes is biased against stars showing weaker activity, thus overestimating the time spent in the violent ejection stage and hence the over-all effect of mass loss. Therefore, it must be kept in mind that the discussion to follow tends to overestimate the effect of mass loss. Let us further assume that all the stars represented in the statistics have roughly the same mass, and consider two representative values, 1.5 $m_\odot$ and 1.0 $m_\odot$. The normal contraction times are then about 1.17×10^7 years and 3.01×10^7 years, respectively (Iben 1963) to reach the vicinity of

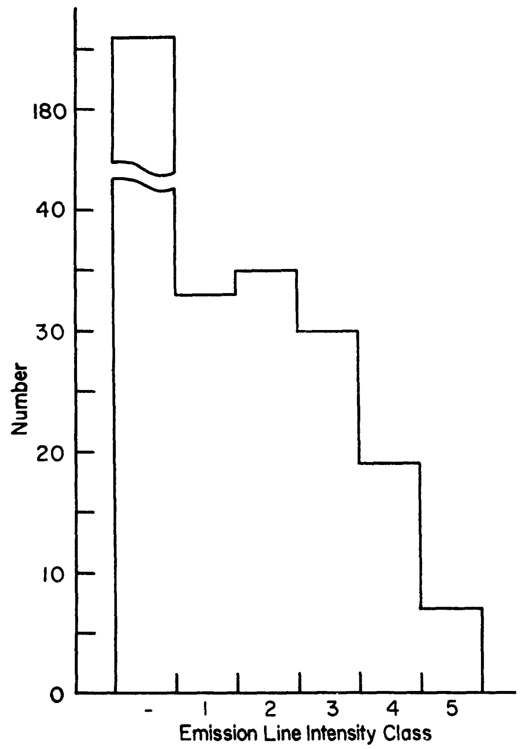

FIG 12.—Number of known T Tauri stars brighter than $m_{pg} = 14.5$ as a function of emission-line intensity class

the main sequence. We may further assume that either (*case a*) the ejection is most violent initially but dies down gradually, passing through each of the emission-line intensity classes in turn and ejecting at the respective mean rate while in those classes; or (*case b*) the ejection takes place with some mean rate obtained from the data of Table 12. This does not necessarily imply continuous ejection but simply that there is some applicable average rate. Both cases will be assumed to occur with a constant ejection velocity during the initial 40 per cent of the star's contractive time, i.e., the T Tauri stage.

We may now determine the modified contraction times and the total mass lost if the average rates apply. Table 13 lists the detailed results for a 1.5 $m_\odot$ star ejecting according to *case a*. The luminosity L, the radius R, and the contraction rate dR/dt are from Iben; the rates of mass ejection dm/dt have been obtained from the present results; $b dm/dt$ represents the energy involved in the ejection; τ is the time elapsed on the modified contraction time scale, and Δm is the total mass lost up to time τ. Although the over-all effect on the time scale seems negligible (1.0 per cent, or 35.36×10^{13} sec with mass loss as compared to 35.95×10^{13} sec without) the mass lost is a substantial fraction of the total: 0.17 $m_\odot$ or 11 per cent. It is also important to note that the mass-loss term is at times as great as about 16 per cent of the radiative luminosity, thus implying that energy transfer by means of mass ejection may have to be considered in the construction of pre-main-sequence evolutionary models. Under *case b*, continuous ejection at a constant rate of 2.3×10^{18} gm sec^{-1} results in a total mass loss of 0.16 $m_\odot$ and a 2.2 per cent shorter contraction time.

Table 14 shows the results for a 1.0 $m_\odot$ star assuming *case a* and that the same average

TABLE 13

EFFECT OF MASS LOSS IN *Case a*

(m = 1 5 $m_\odot$)

L (10^{34} erg sec^{-1})	R (10^{11} cm)	dR/dt (10^{-3} cm sec^{-1})	bdm/dt (10^{34} erg sec^{-1})	τ (10^{13} sec)	Δm (10^{31} gm)
3 55	3 84	22 2	0 394	0 147	1 21
2 97	3 42	15 15	394	0 387	3 39
2 43	3 08	9 85	394	0 677	5 93
2 00	2 76	6 42	225	1 131	8 20
1 63	2 46	4 15	225	1 722	11 16
1 37	2 21	2 66	225	2 413	14 61
1 18.	2 04	1 93	141	2 985	16 39
1 018	1 89	1 34	141	4 143	20 00
0 900	1 735	0 868	141	5 544	24 37
0 814	1 610	0 550	0842	7 314	27 68
0 777	1 529	0 437	0842	8 92	30 69
0 790	1 458	0 180	0281	11 27	32 16
0 860	1 430	0 049	0 0281	13 79	33 74
					= 0 17 $m_\odot$

TABLE 14

EFFECT OF MASS LOSS IN *Case a*

(m = 1 0 $m_\odot$)

L (10^{34} erg sec^{-1})	R (10^{11} cm)	dR/dt (10^{-3} cm sec^{-1})	bdm/dt (10^{34} erg sec^{-1})	τ (10^{13} sec)	Δm (10^{31} gm)
2 33	3 47	80 4	0 394	0 043	0 38
1 90	3 09	17 2	394	0 220	1 93
1 53	2 76	10 84	394	0 456	4 00
1 23.	2 43	7 09	394	0 769	6 74
0 987	2 13	4 45	394	1 185	10 38
0 791	1 92	2 75	394	1 720	15 06
0 630	1 77	1 79	225	2 552	19 22
0 499	1 52	1 080	225	3 662	24 77
0 399	1 358	0 686	225	5 089	31 91
0 320	1 214	0 437	141	7 18	38 44
0 287	1 096	0 266	141	9 79	46 59
0 246	1 001	0 164	141	13 05	56 76
0 196	0 929	0 1012	0842	17 44	64 96
0 182	0 874	0 0677	0842	22 36	74 16
0 183	0 831	0 0435	0 0281	29 28	78 48
					= 0 40 $m_\odot$

rates apply. Here the effects are much more serious: the time scale is shortened by 9 per cent, but the mass lost is 0.40 $m_\odot$, almost one-half the star's initial mass. The mass-loss term also becomes as large as 57 per cent of the radiative luminosity so that it clearly can no longer be neglected. *Case b* gives a mass loss of 0.34 $m_\odot$ with a 10 per cent shortening of the time scale.

The extremely large fraction of mass lost causes one to consider the possibility that the ejection might be proportional to the mass of the star, and hence that a 1.0 $m_\odot$ star would not actually eject 0.4 of its mass. Table 15 lists the masses of the stars observed as determined from the escape velocities, which result from the theory of the emission profiles, and the observed ejection rates. There is a rough correlation in the expected direction, i.e., the more massive stars have the largest ejection rates. However this conclusion needs to be strengthened by more observational data. If the suggested correlation is accepted, and we repeat the previous calculations with a lower ejection rate (1.5×10^{18} gm sec^{-1}) for *case b*, we find that the total mass loss is reduced (to 0.24 $m_\odot$) and the effect on the time scale is only 6 per cent. But again the indication is that mass loss is of importance.

TABLE 15

MASSES AND EJECTION RATES

Star	v_∞ (km/sec)	$R_0/R_\odot$	$m/m_\odot$	dm/dt (10^{-7} $m_\odot$ yr^{-1})
LkHα 120	375	11 16	4 10	5 85
RU Lup .	429	2 95	1 42	1 42
GW Ori	240	8 64	1 30	0 35
RY Tau	325	3 25	0 90	0 31
AS 209	325	2 94	0 81	0 65
T Tau	225	4 56	0 60	0 35

It must be emphasized again that the above results are likely to be overestimates because of the assumptions involved in the interpretation of the statistical data. It is also a great risk to generalize from observational results for only six stars observed at one time, to the whole group of contracting stars considered over their contractive lifetimes. The general trends might be considered to be more safely established than the detailed results. That is to say, it appears that mass ejection at the rates found here decreases the contraction time scales by non-negligible amounts, and its inclusion in detailed evolutionary computations seems to be indicated.

VII. THE ROLE OF T TAURI MASS EJECTION OF A GALACTIC SCALE

We now consider the role mass ejection from T Tauri stars plays in the over-all mass balance of the interstellar medium. It was estimated that about 40 per cent of the stars of the "Orion population" are ejecting matter in varying amounts, with an average rate of 3.7×10^{-8} $m_\odot$ per year. From the available statistics on the number of faint Hα-emission stars brighter than $M_{pg} = +11.25$ in the major concentrations (the Orion Nebula, NGC 2264, NGC 7000, and IC 5070) Herbig (1962) has estimated that the total number of Orion population stars within 1 kpc of the Sun is at least 12000. This corresponds to an average space density of 2.9×10^3 star kpc^{-3} for the solar neighborhood.

If we represent the galaxy by a disk of radius 15 kpc and thickness 0.5 kpc and assume that the above-average density applies to the galaxy as a whole, then the total number of T Tauri stars is 10^6. Then, if our average rate of mass loss is valid, the total mass ejected per year throughout the galaxy is 0.04 $m_\odot$. If the ejection has occurred at the same rate over the lifetime of the galaxy (10^{10} years) and the number of T Tauri stars has remained roughly constant, this amounts to 4×10^8 $m_\odot$, or 8 per cent of the present mass of the interstellar medium. Therefore, at current rates of ejection it does not seem likely that the ejected material represents a significant proportion of the interstellar medium. This is also indicated by Biermann's (1955) estimates that the other sources of mass loss (supernovae, novae, Wolf-Rayet stars, supergiants, corpuscular emission, etc.) amount to 1–10 $m_\odot$ per year, two orders of magnitude larger than the contribution from T Tauri stars.

However, in localized regions such as the Orion Nebula the situation may be somewhat different. A 10 per cent loss in mass must involve a drastic change in a star's structure because of the density distribution. According to Schwarzschild (1958) a star of 1 $m_\odot$ contains 90 per cent of its mass within 50 per cent of its radius. Therefore, if the 10 per cent lost comes primarily from the outer regions of the star and in particular from the surface layers which are lithium-rich, the net result should be a decreasing lithium content in the stellar atmosphere during contraction. If the lithium were produced by surface reactions, then the loss of this material could be expected to increase the interstellar lithium concentration in regions where stars have recently formed, as in Orion, the Taurus clouds, etc. However, the degree of enrichment would be difficult to estimate and is likely to be rather small.

VIII. SUMMARY

Within the limitations of the model, the estimated mass losses range from 0.31 to 5.85×10^{-7} $m_\odot$ per year with a weighted mean rate of 3.7×10^{-8} $m_\odot$ per year, the velocities of ejection being from 225 to 325 km/sec. The discrepancies in detailed agreement of the profiles indicate that the ejection may be non-uniform and variable with time.

The net effect of mass ejection on the time scale of contraction does not seem to be very great. A 1.5-$m_\odot$ star ejecting mass for about 40 per cent of its contractive life shortens that life by $\sim$2 per cent; a 1.0 $m_\odot$ star undergoing ejection at the same rate shortens its contractive life by $\sim$10 per cent. This would contribute to the spread in position of contracting stars above the main sequence in color-magnitude diagrams of very young clusters.

However, the effects of such large mass loss (0.17 $m_\odot$ and 0.40 $m_\odot$ for 1.5-$m_\odot$ and 1.0-$m_\odot$ stars, respectively) on the individual stars must be rather drastic. The energies involved in the ejection are comparable to the radiative luminosity (as much as 10–50 per cent) and thus constitute an alternative mode of energy transport. In addition, the internal structure of the star must undergo rather large changes to accommodate such ejection. However, detailed consideration of this phenomenon will have to await more elaborate calculations in which mass loss has been included.

The suggestion that high-energy protons may be responsible for both the large extent of the ionized region surrounding the star and the ejection itself seems attractive. The particle flux required is considerably smaller than that postulated by Fowler, Greenstein, and Hoyle for surface spallation reactions, so from this fact one might suspect that mass ejection may follow the phase of lithium production in T Tauri stars.

The contribution of T Tauri mass loss to the interstellar medium does not appear significant on a galactic scale since the total mass involved is only a few per cent of that of the present interstellar medium.

Therefore, it must be concluded that the over-all effect of mass ejection on the contraction stage of stellar evolution does not appear to be very great, especially since the rates obtained here are at best upper limits if they are representative at all. However, an individual star may be rather seriously affected by mass ejection, and therefore it seems necessary to include the effect in evolutionary computations.

I would like to express my sincere appreciation to Dr. G. H. Herbig for his guidance and encouragement through this work and to Dr. A. E. Whitford for the facilities made available to me at Lick Observatory. I am also greatly indebted to Drs. G. H. Herbig and G. W. Preston for providing the necessary spectra, to Dr. I. Iben for the use of unpublished data, and to Drs. G. F. Chew, C. Hayashi, L. G. Henyey, C. R. O'Dell, and J. G. Phillips for helpful comments and suggestions.

I would also like to thank the National Science Foundation for its support during this investigation.

REFERENCES

Aller, L. H. 1956, *Gaseous Nebulae* (London: Chapman & Hall, Ltd).
Babcock, H. W. 1958, *Ap. J. Suppl* , **4**, 141.
Badalian, H. S. 1958, *Soob. Biurakan Obs* , No. 25, 49.
Baker, J. G., and Menzel, D. H. 1938, *Ap J.*, **88**, 52
Biermann, L. 1955, *Gas Dynamics of Cosmic Clouds* (Amsterdam: North-Holland Publishing Co.), p. 212.
Burgess, A. 1958, *M.N.*, **118**, 477.
Chandrasekhar, S. 1934, *M.N.*, **94**, 534.
Fowler, W. A., Greenstein, J. L., and Hoyle F 1962, *Geophys. J. R Astr. Soc* , **6**, 148.
Herbig, G. H. 1950, *Ap. J.*, **111**, 11.
———. 1957, *ibid.*, **125**, 612.
———. 1958, *Mém. Soc. R. Sci Liège*, 4th ser , **18**, 251
———. 1960, *Symposium on Stellar Evolution* (La Plata), p. 23
———. 1961, *Ap. J.*, **133**, 337.
———. 1962, *Advances in Astronomy and Astrophysics*, **1**, ed Z Kopal (New York: Academic Press), p. 47.
Hoyle, F. 1960, *Quart J. R. Astr. Soc* , **1**, 28.
Iben, I. 1963, private communication.
Joy, A. H. 1945, *Ap. J* , **102**, 168
———. 1949, *ibid* , **110**, 424
Kholopov, P. N. 1954, *Vanderl. Sterne*, **10**, 180
———. 1961, *ibid.*, **13**, 430.
Osterbrock, D. E 1958, *Pub. A S P.*, **70**, 399.
Rottenberg, J. A. 1952, *M.N* , **112**, 126.
Rublev, S. V. 1961, *Soviet Astr —A J* , **4**, 780.
Sanford, R. F 1947, *Pub. A.S P* , **59**, 134
Schwarzschild, M. 1958, *Structure and Evolution of the Stars* (Princeton, N J : Princeton University Press).
Smak, J. 1964, *Ap. J.*, **139**, 1095.
Sobolev, V. V 1960, *Moving Envelopes of Stars*, trans. S Gaposchkin (Cambridge, Mass : Harvard University Press).
Varsavsky, C. M 1960, *Symposium on Stellar Evolution* (La Plata), p 33
Walker, M. F. 1956, *Ap. J Suppl* , **2**, 365.
———. 1957, *Ap. J.*, **125**, 636.
Weston, E. B , and Aller, L. H. 1955, *Mém Soc. R. Sci Liège*, 4th ser., **15**, 251.
Wood, D. B. 1963, unpublished Ph D dissertation, University of California
Wright, K O 1951, *Pub D A O* , Victoria, **9**, 167.